

## Thermophysical and Transport Properties of the BaCl<sub>2</sub>-CsCl High Temperature Ionic Liquid Mixtures

Ana-Maria Popescu<sup>✉</sup><sup>a</sup> and Virgil Constantin<sup>✉</sup><sup>\*,a</sup>

<sup>a</sup>Ilie Murgulescu Institute of Physical Chemistry of the Romanian Academy,  
Splaiul Independentei 202, 060023 Bucharest, Romania

High temperature ionic liquids (HTILs) densities and transport properties for mixtures BaCl<sub>2</sub>-CsCl,  $x(\text{BaCl}_2) = 0-1$ , have been studied as a function of composition and temperature. In terms of Arrhenius theory, the temperature correlation of all measured properties was made and discussed. Thermodynamic properties (isothermal compressibility, molecular volume, lattice energy, heat capacity, molar Gibbs energy, enthalpy and entropy) were derived for all the studied HTILs from experimental data. The viscosity isotherms show negative deviations from linearity, while conductivity isotherms have positive deviations which may be related to the formation of highly negative charged ion associated species. The evolution of the excess quantities: viscosity deviation ( $\Delta\eta$ ), excess molar viscosity ( $\Delta E_\eta$ ), excess molar conductivity ( $\Delta E_\kappa$ ), show a very good parallelism. The linear behavior between conductivity and viscosity was determined using the fractional Walden rule and the average slope was found far from unity.

**Keywords:** high temperature ionic liquids, BaCl<sub>2</sub>-CsCl, binary mixture, density, thermodynamic properties, transport properties

### Introduction

High temperature ionic liquids (HTILs) are an excellent medium for storage, chemical reaction and energy transfer.<sup>1,2</sup> New trend in innovative technologies should be developed to recover metals from secondary resources (waste). The advantages of HTILs are low vapor pressure, thermal stability, high heat capacity and good applications in metallurgical industries, fuel cells, nuclear energy, etc.<sup>3</sup> The oxygen and water-free HTILs electrolysis conditions also provide an excellent working environment for metal processing. HTILs represent the only class of dissociated liquids in positively and negatively charged ionic species in the absence of any dielectric medium.<sup>4</sup> Under the conditions of direct contact between the ions of opposite charges, strong electrostatic attraction forces are exerted, which materialize at the level of the entire melt through a local arrangement ordered similar to that of the ionic crystals. However, the melting takes place, in most cases, with an increase in volume of 10-30% accompanied by a decrease in the interionic distance and a reduction in the average number of particles in the first sphere of coordination, which proves that compared to the solid from which comes, in the melt there is an excess

of “free volume”, which favors fluidity.<sup>5</sup> Although the ions present in the melt do not occupy fixed lattice positions and their translational movement is facilitated by the excess of free volume, they cannot still move independently of each other due to the interaction forces exerted between them.<sup>6</sup> It follows that these forces directly govern the transport properties of the melts and their study can provide some of the most interesting structural data.

The study of the specialized literature in the field of physical chemistry of HTILs led to the very interesting conclusion that most of the information we currently have about the nature of ionic interactions in this class of substances was obtained from studies undertaken on the transport coefficients in this class of ionic liquids.<sup>7</sup> In fact, no technological use of HTILs can be imagined without knowing their transport properties (viscosity and conductivity). And since viscosity is directly related to HTILs density, and density to a number of important thermodynamic parameters, it is clear that any study of transport properties must include the study of density. The present paper aims a systematic study of the density (along with derived thermodynamic properties), viscosity and electrical conductivity in binary HTILs mixtures BaCl<sub>2</sub>-CsCl in order to complete the table of physico-chemical data necessary for new technological application (nuclear science/pyroprocessing) of this system and to obtain additional information on ionic interactions and

\*e-mail: virgilconstantin@yahoo.com

Editors handled this article: José Walkimar M. Carneiro and Fernando C. Giacomelli (Associate)

so elucidating their structure. We performed this study of the BaCl<sub>2</sub>-CsCl mixture,  $x(\text{BaCl}_2) = 0-1$  in a wide temperature range over the entire concentration range.

## Experimental

### Chemicals and preparation of HTILs mixtures

The mixtures were prepared by using commercially available BaCl<sub>2</sub> and CsCl reagents Merck KGaA (Darmstadt, Germany) and Alpha Aesar (Ward Hill, Massachusetts, USA) of 99.9% purity, which after double recrystallization from distilled water were dried at least for 48 h at 423.15 K and then melted under special conditions to remove any compound formed by hydrolysis upon heating. A quartz cell previously established in our laboratory<sup>8</sup> was used for this purpose. The crystallized salt contained in a quartz tube was slightly heated to melting temperature, alternately in vacuum or in an atmosphere of dry argon saturated with CCl<sub>4</sub> vapors. After melting, the gas is bubbled through the melt for 1.5 h. Chlorine obtained by decomposition of CCl<sub>4</sub> vapors at cell temperature proved to be a very active purifying agent. By a change in the gas pressure in the cell, the melt is evacuated through a capillary into a vessel where it is quenched with CCl<sub>4</sub> (cooled in ice), in the form of solid pearls. By choosing the convenient pressure, pearls of the desired size can be obtained, so that the subsequent handling can be done easily. The salt thus obtained was always controlled with phenolphthalein in terms of alkalinity. The salt was then stored in a desiccator under CCl<sub>4</sub> and subsequent handling was done in a dry box. In all cases, the mixtures were prepared in a dry box, with less than 5 ppm of O<sub>2</sub> and H<sub>2</sub>O, by weighing the previously melted pure components.

### Apparatus and procedure

For the BaCl<sub>2</sub>-CsCl mixtures at temperatures between 963.65 and 1348.15 K were measured density ( $\rho$ ), viscosity ( $\eta$ ) and electrical conductivity ( $k$ ). The classical method using Archimedes' principle was used for density measurements, using laboratory equipment already tested and calibrated for measurements in molten salts.<sup>9,10</sup> The uncertainty limit of the Archimedean technique is within  $\pm 0.02 \text{ kg m}^{-3}$ .<sup>11</sup> Details on this technique were presented elsewhere.<sup>12,13</sup> The viscosity measurement was performed with the previously developed oscillating sphere method, displaying a precision of  $\pm (2-3\%)$ .<sup>11</sup> Details on this technique were presented elsewhere.<sup>10,13-15</sup> For both experimental measurement, density and viscosity, were used vertical furnaces working in argon controlled atmosphere. A constant temperature of the furnace within  $\pm 0.2 \text{ }^\circ\text{C}$  was ensured during measurements. Any

contact with atmosphere oxygen and humidity was avoided and permanent flow of thoroughly dried argon gas free of oxygen was passed inside the furnaces during experiments. Using a thermocouple Pt-Pt/Rh and a thermoregulator we controlled the furnace temperature constant. A capillary quartz cell with four platinum cylindrical electrodes was used for conductivity measurements as described in previous paper.<sup>16</sup> The cell was filled with the system under study and placed in a thermostated electrical four in order to obtain a constant and controllable temperature. After salts melting, conductivity of the HTILs was measured with the conductivity meter Radiometer (Copenhagen, Denmark) CDM 230. Experimental runs conducted both upon heating and cooling regimes at a rate of  $1 \text{ K min}^{-1}$  showed reproducibility within 1% of these two series; an average value was used in further calculations. The accuracy of the electrical conductivity measurements was estimated to be  $\pm 2\%$ . A Paragon-Thermocouple (Paragon Industries-London, UK) S-Type (Pt-Rh10/Pt) was used to control the temperature. Experimental cells were calibrated in the same temperature range with pure KCl melt, as described by Janz.<sup>17</sup> All measurements were carried out under argon atmosphere.

## Results and Discussion

### Density

One important physical property of HTILs is the density, on which temperature play a significant role in general. Experimental value of HTILs mixtures BaCl<sub>2</sub>-CsCl (with molar fraction ( $x$ ) reported to BaCl<sub>2</sub>, being: 0, 0.85, 0.72, 0.53, 0.33, 0.12 and 1) in temperature range 963.65-1348.15 K were reported. Additional Tables S1-S7 from the Supplementary Information (SI) section present all experimental data obtained for each composition of the mixture. The density data presented in these tables are plotted in Figure 1.

The correlation with temperature of all experimental density data can be expressed using the following linear equation:

$$\rho = a + (b \times T) \quad (1)$$

expressing the correlation of all experimental density data ( $\rho \text{ (kg m}^{-3}\text{)}$ ) with temperature ( $T \text{ (K)}$ ).

In Table 1 are listed the characteristic parameters from equation 1 ( $a$  and  $b$ ) determined from the intercept and slope, respectively, of the corresponding straight lines from Figure 1. The density of the studied systems (Figure 1 and Table 1) decreases linearly with increasing temperature and decreases from BaCl<sub>2(pure)</sub> to CsCl<sub>1(pure)</sub>.

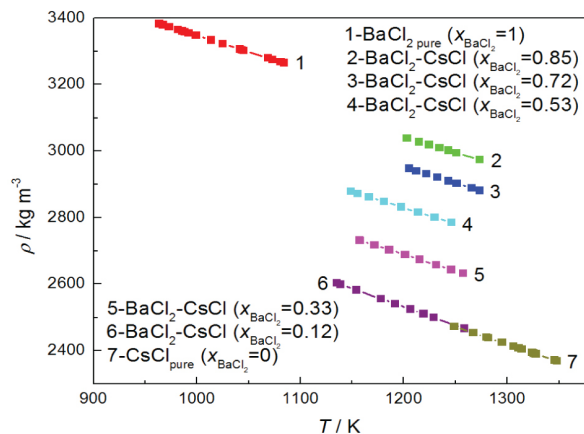


**Figure 1.** Densities vs. temperature for several mole fractions in HTILs mixtures BaCl<sub>2</sub>-CsCl,  $x(\text{BaCl}_2) = 0-1$ .

So, the addition of BaCl<sub>2</sub> to the CsCl has the effect of increasing density of the HTILs mixture. Comparing our results with other old data from literature<sup>17</sup> we found a very good agreement on pure components (absolute relative deviation of 0.24% for CsCl<sub>(pure)</sub> and 0.23% for BaCl<sub>2(pure)</sub>). Due to the above discussed differences for the density of pure components, similar differences are expected for the mixtures investigated. Thus, a comparison with literature data<sup>17</sup> indicated indeed differences of  $\pm 0.26-0.35\%$ .

The density data obtained for the different BaCl<sub>2</sub>-CsCl systems were used for subsequent calculation of different thermodynamic properties, as presented below. The expansion of density with temperature is quantified by thermal expansion coefficient,  $\alpha$ , defined as:

$\alpha = -(1/\rho)(\partial\rho/\partial T)_p$ . This parameter can be calculated by the  $\ln \rho$  vs.  $T$  plot fitted according to a straight line:

$$\ln \rho = c - (\alpha \times T) \quad (2)$$

where  $c$  is an empirical constant ( $\text{kg m}^{-3}$ ).

The data from Table 2 fit well equation 2;  $\alpha$ , in the mixture BaCl<sub>2</sub>-CsCl is found to decrease with increasing CsCl content.

Using equation 3 the molecular volume,  $V_{\text{mol}}$  ( $\text{nm}^3$ ), can be calculated, where  $M$  is the molar mass ( $\text{kg mol}^{-1}$ ) and  $N_A$  the Avogadro's constant ( $6.0221 \times 10^{23} \text{ mol}^{-1}$ ).

$$V_{\text{mol}} = M/(N_A \times \rho) \quad (3)$$

Molar mass for the studied mixture is presented in SI section, Table S8. The lattice energy,  $U_{\text{pot}}$  ( $\text{J mol}^{-1}$ ) was calculated according to the following equation:<sup>18,19</sup>

$$U_{\text{pot}} = \gamma(\rho/M)^{1/3} + \delta \quad (4)$$

where  $\gamma$  is the coefficient  $\gamma = 8375.6$  and  $\delta$  is the coefficient  $\delta = -178.8$ .

Isothermal compressibility,  $\beta$  in  $\text{Pa}^{-1}$ , was calculated according to the following equation:<sup>18,19</sup>

$$\beta = k'' \times V_{\text{mol}} \quad (5)$$

where the coefficient  $k'' = 0.159$ .

**Table 1.** Coefficients of equation 1 (a, b), together with standard deviation ( $\sigma$ ), correlation factors (adj.  $R^2 = 0.999-1$ ) along with temperature range, for HTILs mixtures BaCl<sub>2</sub>-CsCl;  $x(\text{BaCl}_2) = 0-1$

$x(\text{BaCl}_2)$ / mole fraction	a	$\sigma$	b	$\sigma$	Temperature / K
1	4329.25	1.47	-0.9819	$1.40 \times 10^{-3}$	963.65-1084.15
0.85	4139.13	0.41	-0.9149	$3.35 \times 10^{-4}$	1203.15-1273.65
0.72	4115.63	1.98	-0.9692	$1.60 \times 10^{-3}$	1205.15-1273.65
0.53	3986.72	2.54	-0.964	$2.10 \times 10^{-3}$	1149.15-1246.15
0.33	3886.53	0.37	-0.9975	$3.09 \times 10^{-4}$	1157.15-1257.65
0.12	3859.64	0.38	-1.1067	$3.19 \times 10^{-4}$	1135.35-1258.65
0	3781.03	0.36	-1.0475	$2.80 \times 10^{-4}$	1248.75-1348.15

**Table 2.** Coefficients of equation 2 at 1050 K, together with standard deviation ( $\sigma$ ), correlation factors (adj.  $R^2 = 0.999-1$ ) along with temperature range, for HTILs mixtures BaCl<sub>2</sub>-CsCl;  $x(\text{BaCl}_2) = 0-1$

$x(\text{BaCl}_2)$ / mole fraction	$c$ / ( $\text{kg m}^{-3}$ )	$\sigma$	$\alpha$ / $\text{K}^{-1}$	$\sigma$
0	8.4113	$4.427 \times 10^{-4}$	$2.9546 \times 10^{-4}$	$4.34 \times 10^{-7}$
0.85	8.3852	$6.084 \times 10^{-4}$	$3.0431 \times 10^{-4}$	$4.93 \times 10^{-7}$
0.72	8.3895	$5.980 \times 10^{-4}$	$3.3257 \times 10^{-4}$	$4.83 \times 10^{-7}$
0.53	8.3562	$1.530 \times 10^{-5}$	$3.4023 \times 10^{-4}$	$1.28 \times 10^{-6}$
0.33	8.3429	$8.879 \times 10^{-4}$	$3.7159 \times 10^{-4}$	$7.37 \times 10^{-7}$
0.12	8.3593	$1.600 \times 10^{-4}$	$4.3575 \times 10^{-4}$	$1.35 \times 10^{-6}$
1	8.3542	$1.040 \times 10^{-3}$	$4.3314 \times 10^{-4}$	$7.96 \times 10^{-7}$

$\alpha$ : thermal expansion coefficient;  $c$ : empirical constant of equation 2.

According to the equation 6,<sup>12</sup> the heat capacity,  $C_p$ , was also calculated, with the coefficients  $k' = 1322$  and  $c' = -0.8$ .

$$C_p / (\text{J K}^{-1} \text{mol}^{-1}) = k' \times V_{\text{mol}} + c' \quad (6)$$

Table 3 present all calculated values from equations 3-6, along with the molar volume at 1050 K for the  $\text{BaCl}_2$ -CsCl,  $x(\text{BaCl}_2) = 0-1$  mixtures. Those data will be used in following explanations.

From Table 3 we can see that molecular and molar volume, isothermal compressibility and heat capacity increase from CsCl to  $\text{BaCl}_2$  in the studied systems, while lattice energy has the opposite behavior. If complex ions are formed in the systems under study, the ion packaging is lower in the mixture than in the pure constituent components and consequently, we expect the mixing to occur with an increase in volume. Taking into account the data in Table 3, the molar volume isotherms were plotted at 1050 K. It was found that the deviations from ideality are very slightly positive, being practically zero. It is very probable that in this case, due to very low differences in the molar volumes of the pure components, the mixing to allow the accommodation of the new complex entities formed without important volume changes.

### Viscosity

Viscosity is an important parameter for the electrolysis process and is an important property for electrochemical studies because it has strongly influenced the mass transport velocity in a solution. Energy requirements for processing these fluids can be reduced by knowing the temperature effect on viscosity.<sup>20</sup> In the SI section available with this paper, Tables S1-S7 present the experimental values of dynamic viscosities function of temperature of all molar fractions of HTILs  $\text{BaCl}_2$ -CsCl,  $x(\text{BaCl}_2) = 0-1$ . Data reported in SI section shows that viscosity values of single HTILs or of mixtures decrease as temperature increase. Increasing temperature results in a decrease in viscosity because a larger temperature means particles have greater thermal

energy and are more easily able to overcome the attractive forces binding them together. So, rising temperature means higher mobility of ions. These viscosity data are plotted in Figure S1, SI section. As can be seen from this graph, the highest viscosity has  $\text{BaCl}_2$  and the lowest CsCl, while in all the mixtures studied as long as the concentration of CsCl in the mixture decreases, the viscosity of the mixture decreases and its dependence on temperature becomes slower. The agreement between this work and previously mentioned publications<sup>17</sup> on pure components gave us the results of absolute relative deviation of +22.7% for  $\text{CsCl}_{(\text{pure})}$  and +2.46% for  $\text{BaCl}_{2(\text{pure})}$ . For the mixtures, results indicate differences of  $\pm 4-5\%$ . In general, HTILs have exponential decaying viscosity-temperature profiles.<sup>21-23</sup> For both two pure HTILs ( $\text{BaCl}_2$  and CsCl) as long as for the five mixtures, the temperature and viscosity dependence can be well described by the Arrhenius equation:<sup>24</sup>

$$\eta = A_\eta \times \exp(-E_\eta/R \times T) \quad (7)$$

where  $A_\eta$  is the pre-exponential constant,  $A_\eta = \ln \eta_0$  (Pa s),  $\eta_0$  is a constant;  $E_\eta$ : energy of activation for the viscous flow, ( $\text{J mol}^{-1}$ ) and R universal gas constant,  $8.314 \text{ J K}^{-1} \text{ mol}^{-1}$ .

From the following equation:

$$\ln \eta = \ln \eta_0 + (E_\eta/R \times T) \quad (8)$$

whose two parameters ( $A_\eta$  and  $E_\eta$ ) can be calculated.

So, the slopes of the straight lines presented in Figure 2 can be used to determine the activation energies for the viscous flow ( $E_\eta$ ) in all the studied HTILs.

In order to determine the activation energies for the viscous flow ( $E_\eta$ ) in all the studied HTILs one can use the slopes of the straight lines from Figure 2. The calculated pre-exponential factor  $A_\eta$  ( $A_\eta = \ln \eta_0$ ) and activation energies,  $E_\eta$ , for the studied HTILs, along with the regression correlation coefficients (adj.  $R^2$ ) are presented in Table 4. These coefficients have values higher than 0.99 for all HTILs, showing a very good fit.  $E_\eta$  values for the studied mixtures was found to be considerably larger than those for common HTILs.<sup>25</sup>

**Table 3.** The calculated values of the physical quantities in the equations 3-6 for HTILs mixtures  $\text{BaCl}_2$ -CsCl;  $x(\text{BaCl}_2) = 0-1$

$x(\text{BaCl}_2) / \text{mole fraction}$	$V_{\text{mol}} / \text{nm}^3$	$V_M \times 10^3 / (\text{m}^3 \text{mol}^{-1})$	$U_{\text{pot}} / (\text{kJ mol}^{-1})$	$\beta / (\text{G Pa}^{-1})$	$C_p / (\text{J K}^{-1} \text{mol}^{-1})$
0	0.0850	0.0510	22.3775	0.0135	111.2558
0.85	0.1057	0.0636	20.7813	0.0168	138.8869
0.72	0.1056	0.0636	20.7834	0.0168	138.844
0.53	0.1058	0.0637	20.7732	0.0168	139.0484
0.33	0.1062	0.0639	20.7483	0.0169	139.5498
0.12	0.1066	0.0642	20.721	0.0169	140.1002
1	0.1029	0.0777	19.4354	0.0205	169.6950

$V_{\text{mol}}$ : molecular volume;  $V_M$ : molar volume;  $U_{\text{pot}}$ : lattice energy;  $\beta$ : isothermal compressibility;  $C_p$ : heat capacity.

**Table 4.** Calculated pre-exponential factors A<sub>η</sub> and E<sub>η</sub> from equation 7 along with the standard deviation (σ) and temperature ranges for the BaCl<sub>2</sub>-CsCl mixtures, (adj. R<sup>2</sup> = 0.972-0.998); x(BaCl<sub>2</sub>) = 0-1

x(BaCl <sub>2</sub> ) / mole fraction	A <sub>η</sub> × 10 <sup>5</sup> / (Pa s)	σ	E <sub>η</sub> / (kJ mol <sup>-1</sup> )	σ	Temperature / K
1	10.675	0.059	36.801	76.519	0.996
0.85	9.4436	0.248	36.604	306.031	0.972
0.72	6.8408	0.093	38.080	114.991	0.996
0.53	7.5840	0.055	33.301	65.866	0.998
0.33	6.3743	0.062	31.629	74.414	0.997
0.12	8.0944	0.037	25.161	44.242	0.998
0	8.562	0.042	22.464	42.358	0.996

A<sub>η</sub>: pre-exponential constant; E<sub>η</sub>: energy of activation for the viscous flow.

Finally, Arrhenius equations of viscosity are presented for all studied mixtures:

$$x(\text{BaCl}_2) = 0; \ln \eta = 8.5621 \times 10^{-5} + 22464.11(1/T) \quad (9)$$

$$x(\text{BaCl}_2) = 0.85; \ln \eta = 9.4437 \times 10^{-5} + 36604.056(1/T) \quad (10)$$

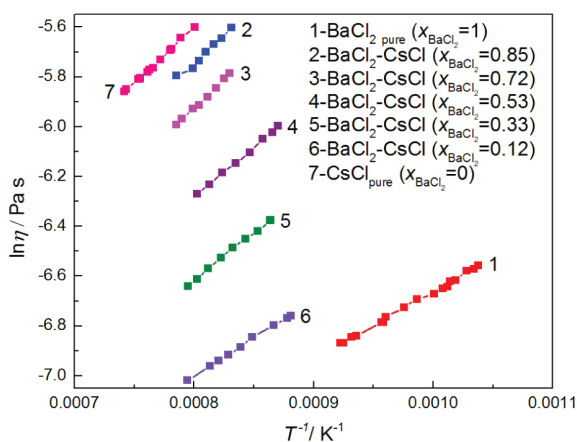
$$x(\text{BaCl}_2) = 0.72; \ln \eta = 6.8408 \times 10^{-5} + 38080.2909(1/T) \quad (11)$$

$$x(\text{BaCl}_2) = 0.53; \ln \eta = 7.5841 \times 10^{-5} + 33301.0571(1/T) \quad (12)$$

$$x(\text{BaCl}_2) = 0.33; \ln \eta = 6.3743 \times 10^{-5} + 31629.8608(1/T) \quad (13)$$

$$x(\text{BaCl}_2) = 0.12; \ln \eta = 8.0944 \times 10^{-5} + 25160.8858(1/T) \quad (14)$$

$$x(\text{BaCl}_2) = 1; \ln \eta = 1.0675 \times 10^{-4} + 36800.8913(1/T) \quad (15)$$

**Figure 2.** Variation of  $\ln \eta$  vs.  $T^{-1}$  in HTILs mixtures BaCl<sub>2</sub>-CsCl; x(BaCl<sub>2</sub>) = 0-1.

For better understanding of the viscous flow in these HTILs, the thermodynamic function of activation were calculated from the dynamic viscosity values by considering Eyring's transition state theory.<sup>26,27</sup>

The following equation express the absolute approach of Eyring on the dynamic viscosity of a liquid mixture:<sup>26,27</sup>

$$\eta = [(h \times N_A)/V_M] \exp(\Delta G^*/R \times T) \quad (16)$$

where h is the Planck's constant ( $6.626 \times 10^{-34}$  J s) and  $\Delta G^*$  the molar Gibbs energy of activation of viscous flow (J mol<sup>-1</sup>).

V<sub>M</sub> of the eutectic mixture, calculated as the ratio of average molar mass and density of the mixture is

presented in Table S8, SI section, and  $\Delta G^*$ , calculated from equation 17. Combining equation 16 with:

$$\Delta G^* = \Delta H^* - (T \times \Delta S^*) \quad (17)$$

yields the equation:

$$\ln[(\eta \times V_M)/(h \times N_A)] = (\Delta H^*/R \times T) - (\Delta S^*/R) \quad (18)$$

where  $\Delta H^*$  is the enthalpy of activation of viscous flow, (J mol<sup>-1</sup>) and  $\Delta S^*$  is the entropy of activation of viscous flow, (J mol<sup>-1</sup>).

$\ln(\eta \times V_M/h \times N_A)$  as a function of  $1/T$  has been calculated and plotted in Figure 3 for each molar fraction of the investigated HTILs, using experimental density and viscosity data obtained.

By plotting data from equation 18 we obtained straight lines. From their slopes and intercepts the enthalpy ( $\Delta H^*$ ) and entropy ( $\Delta S^*$ ) of activation of viscous flow were estimated. Value of  $\Delta G^*$ ,  $\Delta H^*$  and  $\Delta S^*$  are presented in Table 5 and show for all of them a decrease with increasing the CsCl content in the mixtures.

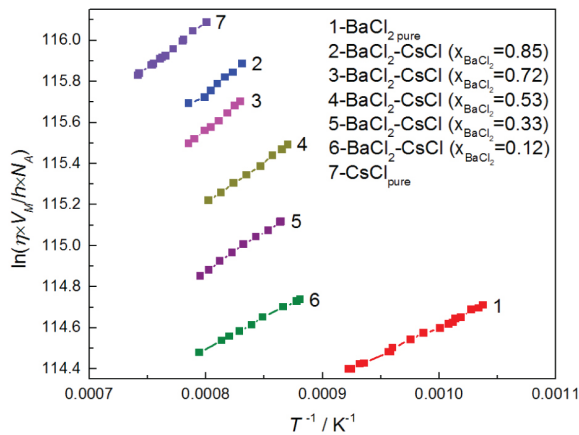
In this system the phase diagram<sup>17,28</sup> presented in Figure S2, SI section, signals the presence of complex combinations of formula BaCl<sub>2</sub>·2CsCl and BaCl<sub>2</sub>·CsCl that melt congruently.

It is clear that in this system the  $Z^+/r^+$  ionic potential of the alkaline cation (Z is the ionic charge and r<sup>+</sup> the cation size) is high and therefore the ionic interactions (Coulomb and polarization) that take place in mixing are high, leading to the formation in the HTILs structure of new entities of [BaCl<sub>4</sub>]<sup>2-</sup> and [BaCl<sub>3</sub>]<sup>-</sup> complex ion structure. A preferential coordination of Cl<sup>-</sup> ions around Ba<sup>2+</sup> ion with formation of BaCl<sub>3</sub><sup>-</sup> complex ions was also postulated by Roewer and Emons<sup>29</sup> from determinations of transport numbers. Papatheodorou and Ostvold's<sup>30</sup> thermodynamic studies show that the tendency of the bivalent ion to associate with the anion is weak in the case of systems containing BaCl<sub>2</sub>, so consequently the stability of [BaCl<sub>4</sub>]<sup>2-</sup> and [BaCl<sub>3</sub>]<sup>-</sup>

**Table 5.** The thermodynamic function of activation of viscous flow for the HTILs systems BaCl<sub>2</sub>-CsCl,  $x(\text{BaCl}_2) = 0-1$  at  $T = 1050$  K

$x(\text{BaCl}_2)$ / mole fraction	$\Delta H^*$ / (kJ mol <sup>-1</sup> )	$\Delta S^*$ / (kJ mol <sup>-1</sup> )	$\Delta G^*$ / (kJ mol <sup>-1</sup> )
1	38640.9362	0.0135	38626.7235
0.85	38434.2586	0.0135	38420.0867
0.72	39984.3057	0.0135	39970.1745
0.53	34966.1099	0.0135	34951.9655
0.33	33211.3535	0.0135	33197.2306
0.12	26418.9301	0.0135	26404.7765
0	23587.3158	0.0135	23573.1842

$\Delta G^*$ : the molar Gibbs energy of activation of viscous flow;  $\Delta H^*$ : enthalpy of activation of viscous flow;  $\Delta S^*$ : entropy of activation of viscous flow.

**Figure 3.** Plots of  $\ln(\eta \times V_M/h \times N_A)$  against inverse temperature for different mole fraction in HTILs studied.

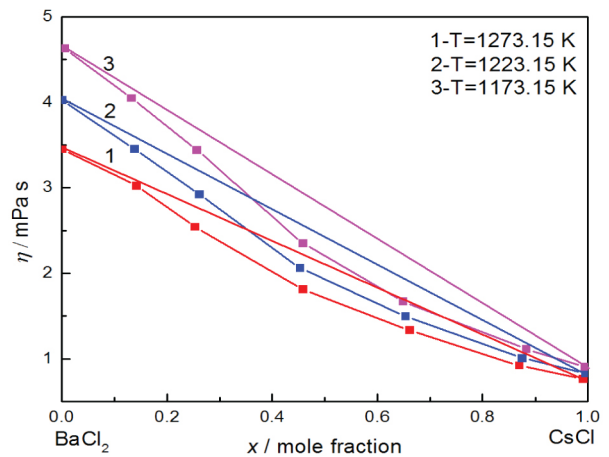
complex ion is lower. At the same time, as it results from the study of the mixing heats carried out by Davis<sup>31</sup> in the BaCl<sub>2</sub>-CsCl system, minimum points appear on the  $\Delta H$  isotherms depending on the composition, which illustrates the tendency of association of the bivalent ion with the Cl<sup>-</sup> anion. The fact that in this system there are changes in the anion-cation bond energy in the mixture, is also confirmed by the evolution of the deviations of the activation energy from additivity:

$$\Delta E_\eta = E_\eta^{\text{exp}} - E_\eta^{\text{id}} \quad (19)$$

$$E_\eta^{\text{id}} = x_1 E_{\eta_1} + x_2 E_{\eta_2} \quad (20)$$

where  $E_\eta^{\text{exp}}$  is the activation energy experimental and  $E_\eta^{\text{id}}$  is the activation energy ideal, proving that in these systems the phenomenon of viscous flow occurs with greater difficulty, most likely due to the formation of new ionic associations following ionic interactions. Figure 4 presents the viscosity isotherms. As can be seen, these isotherms show negative systematic deviations from linearity, which reach values of 20%, thus proving that in this system strong ionic interactions take place when mixed.

As shown in the phase diagram (Figure S2, SI section) the concentration of complex ions presents on this isotherm

**Figure 4.** Viscosity isotherms in the system BaCl<sub>2</sub>-CsCl;  $x(\text{BaCl}_2) = 0-1$ .

curves show a maximum point which proves that this region is difficult to overcome because of the growing of ionic interaction in the mixture. We notice at the same time the perfect parallelism between evolutions of the excess quantities ( $\Delta\eta$  and  $\Delta E_\eta$ ) depending on the composition (Figure 5). This behavior proved that the viscous flow take place with difficulties because of the growing of ionic interaction in the mixture and the formation of  $[\text{BaCl}_3]^-$  complex ions.

#### Electrical conductivity

One of the most important properties of HTILs as electrolyte materials is ionic conductivity. In that condition higher energy efficiency is to be expected when electrolyte with higher conductivity exhibits a lower ohmic drop during electrolysis and so a lower cell voltage. This is the explanation for the importance of conductivity data. The obtained conductivity experimental data for HTILs mixtures BaCl<sub>2</sub>-CsCl,  $x(\text{BaCl}_2) = 0-1$  which lies in the range 1.487-236.8 S m<sup>-1</sup> are given in Table S1-S7 (SI section) and as one can see that increasing temperature conduct to an increase in conductivity. As temperature increases, the energy gained by the molecules in the molten salt or

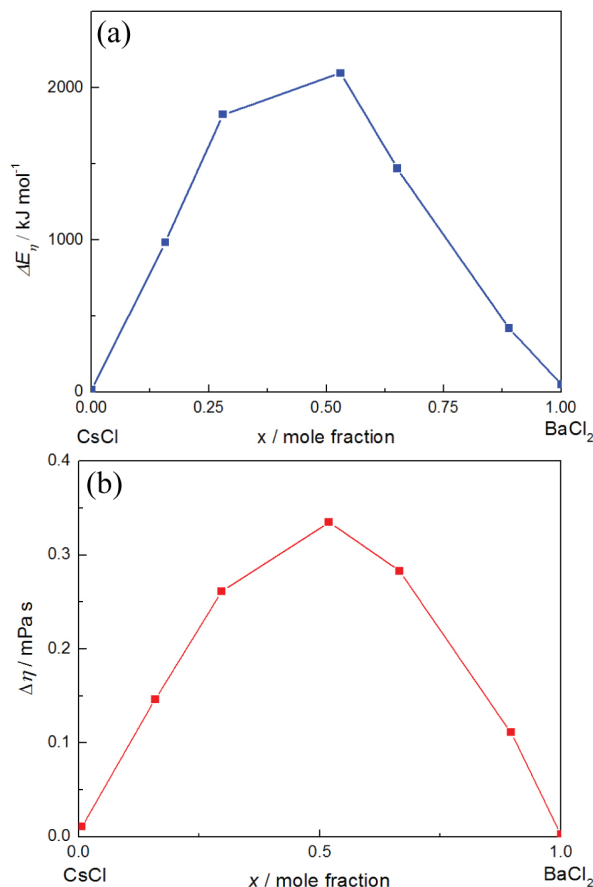


**Figure 5.** Evolution of (a)  $\Delta E_{\eta}$  and (b)  $\Delta \eta$  with the composition of the system BaCl<sub>2</sub>-CsCl;  $x(\text{BaCl}_2) = 0-1$ .

mixture increase and hence the ions are in a higher energy state. This energy will be converted into kinetic energy and so, the mobility of ions increases. Hence the conductivity increases.

Standard deviation of no more than  $\bar{\sigma} = 0.016$  was obtained for the variation of the ionic conductivity ( $k$ ) values with temperature. Taking in account the experimental data we can conclude that those mixtures are highly conducting, thereby confirming that the ionic species are dissociated in the liquid and can move independently. Good agreement was found between obtained data with literature ones<sup>10</sup> and in the limit of  $-2.87\%$ . For CsCl<sub>(pure)</sub> and  $-2.01\%$  for

BaCl<sub>2(pure)</sub>, while for the mixtures the agreement was of  $\pm 2.5-3\%$ .

The following equation was used to fit the specific conductivity obtained data ( $k / \text{S m}^{-1}$ ) for the studied HTILs with Arrhenius equation:

$$\ln k = \ln k_0 - (E_k / R \times T) \quad (21)$$

In that equation the constant called the pre-exponential factor,  $A_k$  is  $\exp(\ln k_0)$  and  $E_k$  is the activation energy for electrical conduction, which indicates the energy needed for an ion to hop to a free hole.

Figure 6 shows that the conductivity data for all studied HTILs fit equation 21 accurately ( $\text{adj. } R^2 = 0.845-0.962$ ). In Table 6 we summarized the values obtained for  $A_k$  and  $E_k$ .

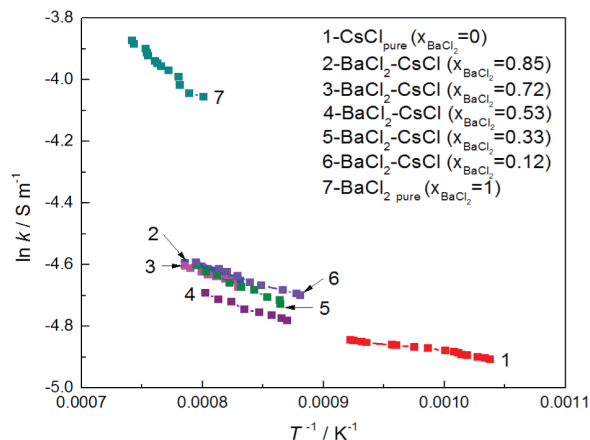


**Figure 6.** Plots of  $\ln$  conductivity vs. reciprocal temperature for the studied mixtures of HTILs BaCl<sub>2</sub>-CsCl;  $x(\text{BaCl}_2) = 0-1$ .

Analogous to viscosity we expect that those results on conductivity to explain the “complexing” occurring in those HTILs. The significant changes in the cation-anion bonding energy on mixing are equally well proved by lower values of  $E_{\eta}$  at the composition where the complex ions are formed. The activation energy has maximum value near composition that corresponds to unstable compounds; in this case  $E_k$  contain parts of energy change involved in the transition from the complex to the single ions.

**Table 6.** Arrhenius equation of conductivity along with the corresponding calculated pre-exponential factors  $A_k$  and  $E_k$ , the standard deviation ( $\sigma$ ) and temperature ranges for the BaCl<sub>2</sub>-CsCl, ( $\text{adj. } R^2 = 0.846-0.971$ );  $x(\text{BaCl}_2) = 0-1$

$x(\text{BaCl}_2) / \text{mole fraction}$	$A_k / (\text{S m}^{-1})$	$\sigma$	$E_k / (\text{kJ mol}^{-1})$	$\sigma$	Temperature / K
0	183.632	0.021	1.647	21.486	963.65-1084.15
0.85	298.103	0.096	7.327	119.082	1203.15-1273.65
0.72	282.799	0.087	6.976	107.999	1205.15-1273.65
0.53	250.394	0.048	6.461	57.104	1149.15-1246.15
0.33	355.861	0.058	9.404	69.598	1157.15-1257.65
0.12	237.516	0.041	5.216	48.482	1135.35-1258.65
1	1560.169	0.111	21.154	145.434	1248.75-1348.15

According to Lumsden's anionic polarization model<sup>32,33</sup> in a binary mixture with common anion  $(M_1-M_2)Cl$  where  $r_1 < r_2$ , the anion is polarized by the asymmetric electric field created by the two cations of different sizes. As a result of this induced anionic polarization a kind of  $M_1-Cl-M_2$  type anion-cation associated groups appear in the melt, the common anion being moved to the smaller cation. As a result, the latter moves in relation to the  $Cl^-$  ion with more difficulty in mixing compared to its pure salt. The ionic mobility being lower, implicitly the electrical conductivity will be lower in the mixture than in the pure salts, because the smallest ion possessing the highest speed is the one that makes the essential contribution to the conductivity of the whole mixture. The effect is more pronounced the greater the difference between the two cations. This theory was also demonstrated in the case of our studied systems  $BaCl_2$ - $CsCl$  with  $x(BaCl_2) = 0-1$ , where  $r(Ba^{2+}) = 135$  nm and  $r(CsCl) = 167$  nm and where it was found to be formed complex ions like  $CsBaCl_3$  and  $Cs_2BaCl_4$  as indicate also the phase diagram (Figure S2, SI section).

So, analogous to viscosity those results on conductivity explain the "complexing" occurring in those HTILs. The significant changes in the cation-anion bonding energy on mixing are equally well proved by lower values of  $E_\eta$  at the composition where the complex ions are formed. The activation energy has maximum value near composition ( $x = 0.33$ ) that corresponds to unstable compounds; in this case  $E_k$  contain parts of energy change involved in the transition from the complex to the single ions.

Also, the large positive excess conductivity activation energy ( $\Delta E_k$ ) is found at almost the composition on which the phase diagram indicates the formation of congruently complex. In the meantime, conductivity isotherms have positive deviations which may be related to the formation of highly negative charged ion associated species such as  $[BaCl_n]^{2-n}$ , ( $n = 4-6$ ). This behavior was also observed by molecular dynamic simulation on chloride complexes formation.<sup>34,35</sup>

The equation 22 gives the relationship between the specific conductance ( $k$ ) and the molar conductivity ( $\Lambda$ ):

$$\Lambda = k \times (M/\rho) \quad (22)$$

In the same time the relation between mobility of ions and viscosity is given by Walden rule ( $\Lambda^\eta = \text{constant}$ ;  $\Lambda$  is the equivalent conductivity). For HTILs it was found that it is more appropriate to use the "fractional Walden rule":

$$\Lambda \times \eta^{\alpha^\#} = c \quad (23)$$

or

$$\log \Lambda = \log c + (\alpha^\# \times \log \eta^{-1}) \quad (24)$$

where  $\alpha^\# = E_\Lambda/E_\eta$  ( $E_\Lambda$  is the activation energy for electrical conduction /  $J \text{ mol}^{-1}$ ) is a positive constant smaller than 1 and  $c$  is a temperature dependent constant.<sup>36-38</sup> The variation of  $\log \Lambda$  vs.  $\log \eta^{-1}$  is represented in Figure 7. In these plots Table 7 presents the values of  $\alpha$  (the slope of the Walden line) and  $c$  (a temperature dependent constant) for  $BaCl_2$ - $CsCl$ ;  $x(BaCl_2) = 0-1$ .

The fact that Walden rule, which proves that the

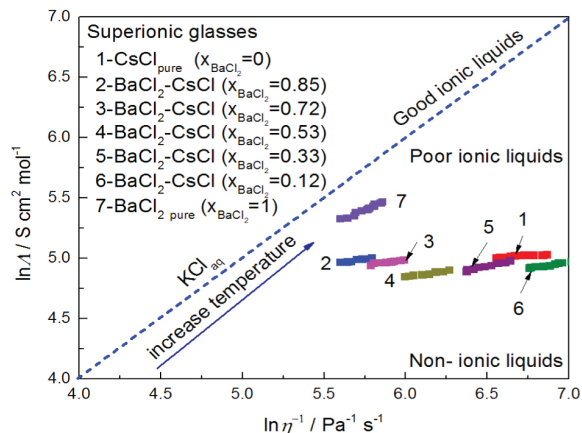


**Figure 7.** Application of fractional Walden rule (equation 24) for the studied HTILs  $BaCl_2$ - $CsCl$ ;  $x(BaCl_2) = 0-1$ .

**Table 7.** Walden equation coefficients with regression coefficients (adj.  $R^2 = 0.958-0.984$ ) along with the standard deviations ( $\sigma$ ) and the temperature range for  $BaCl_2$ - $CsCl$ ;  $x(BaCl_2) = 0-1$

$x(BaCl_2)$ / mole fraction	$\alpha^\# = E_\Lambda/E_\eta$	$\sigma$	$c$	$\sigma$	Temperature / K
1	0.2358	0.181	$27.2214 \times 10^{-5}$	1.043	1248.75-1348.15
0.85	0.0292	0.168	$11.195 \times 10^{-5}$	0.074	1203.15-1273.65
0.72	0.0289	0.138	$11.2135 \times 10^{-5}$	0.081	1205.15-1273.65
0.53	0.0251	0.118	$10.4958 \times 10^{-5}$	0.076	1149.15-1246.15
0.33	0.0376	0.117	$13.8736 \times 10^{-5}$	0.077	1157.15-1257.65
0.12	0.0272	0.107	$10.3439 \times 10^{-5}$	0.073	1135.35-1258.65
0	0.0126	0.176	$4.2129 \times 10^{-5}$	0.033	963.65-1084.15

$\alpha^\# = E_\Lambda/E_\eta$  ( $E_\Lambda$  is the activation energy for electrical conduction and  $E_\eta$ ; energy of activation for the viscous flow) is a positive constant smaller than 1 and  $c$  is a temperature dependent constant.<sup>36-38</sup>

Arrhenius activation energy for conductivity is lower than for viscosity, is applicable in this system shows that one of the ionic species involved is smaller than the other, being able to slip through smaller voids in the condensed phase structure.

Data from Table 7 demonstrate that all the HTILs mixtures BaCl<sub>2</sub>-CsCl,  $x(\text{BaCl}_2) = 0-1$ , obey the fractional Walden rule very well. The values of the Walden slopes are all smaller than unity indicating the presence of obvious ion associations in the investigated HTILs. As all the curves of studied HTILs are positioned under the ideal line in Figure 7.<sup>38</sup> To fix the position of the ideal dotted Walden line in Figure 7, the data for dilute aqueous KCl solution,<sup>39</sup> comprising of equal mobilities of fully dissociated ions,<sup>40</sup> were used. Due to the Walden behavior with different slopes for each mixture studied we can conclude that in the investigated HTILs there are not only charge carrying species (simply formed by Ba<sup>2+</sup>, Cs<sup>+</sup> and Cl<sup>-</sup> ions). So, the conduction involves some degree of cooperation of the ions in question with formation of complex ions. Due to the position of the investigated system of HTILs under the ideal line we can consider them "subionic". The special accumulation structure of these mixtures could generate this phenomenon.

In the case of all HTILs binary systems, the conductivity isotherms show systematic deviations from linearity, the size and shape of these deviations depending directly on the nature of the ions present in the mixture. In binary mixtures with common anion, the excess conductivity ( $\Delta\Lambda$ ) varies in wide limits and is all the greater the difference between the polarization power ( $Z/r^2$ ) of the two cations.<sup>41</sup> It is already known that negative deviation of conductivity from additivity are found in systems in which complex ions are likely to exist in the mixture. The electrical conductivity measurements performed in the KCl-(Ca, Sr, Ba)Cl<sub>2</sub> mixtures showed on the conductivity isotherms the presence of minimums located around the equimolecular compositions, minimums that can be correlated with the formation in melts of complex-coordinated groups that cause a decrease in the actual number of carriers.<sup>41</sup> Thus, representing molar conductivity vs. composition, we found that the obtained curves (Figure 8) are marked by minima within almost the equimolecular composition of the HTILs studied, where phase diagram indicates the formation of congruently melting compound. Correlating our results with others,<sup>34</sup> the above-mentioned behavior can be explained by the formation of the coordinated ionic groups such as  $[\text{BaCl}_n]^{2-n}$ , ( $n = 4-6$ ) which will cause a weakening of ionic packing and will reduce the number of effective current carriers.

At the same time, maximum points appear on the  $E_A$ -composition isotherms as an indication of the more difficult displacement of the bulky ions formed. The excess

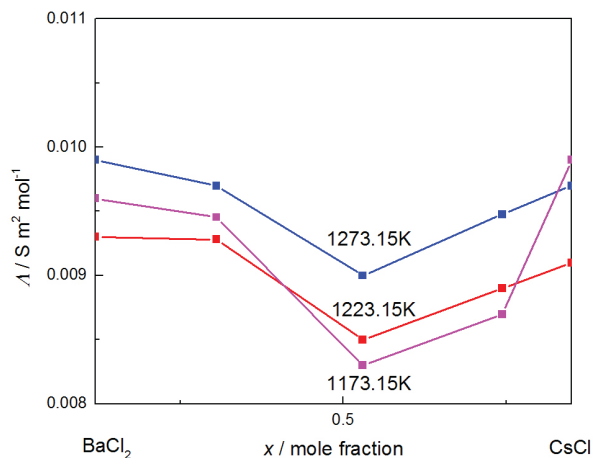


**Figure 8.** Molar conductivity isotherms in the system BaCl<sub>2</sub>-CsCl;  $x(\text{BaCl}_2) = 0-1$ .

molar conductivity ( $\Delta E_k$ ) shows a perfect parallelism with the evolution of the excess quantities ( $\Delta\eta$  and  $\Delta E_\eta$ ) depending on the composition (see Figure 5), proving once again the formation of complex compounds in this system. This behavior proved once again that complex ions can find a wide range of applications in applied chemical engineering.

## Conclusions

The densities, viscosities and electrical conductivities of the HTILs mixtures BaCl<sub>2</sub>-CsCl,  $x(\text{BaCl}_2) = 0-1$ , have been measured as a function of temperature in the range 963.5-1348.15 K at atmospheric pressure. Good transport properties were found for the studied HTILs. Both density and viscosity values decrease with temperature while their conductivities increasing with the same parameter. Classical Arrhenius behavior was found for both viscosity and conductivity values of the investigated HTILs. The strength of the interactions presents in the mixture affect the values of viscosities and conductivities of these HTILs.

The absolute rate approach of Eyring theory concerning the viscosity flow demonstrates for all composition investigated that the interactional factor is predominant over the structural factor.

A lot of thermodynamic data (thermal expansion coefficient, molecular volume, lattice energy and heat capacity) were calculated from the density and viscosity ones. According to the fractional Walden rule, the density, viscosity and conductivity relationship can be set up. The viscosity isotherms show negative deviations from linearity, while conductivity isotherms have positive deviations which may be related to the formation of highly negative charged ion associated species, such as  $[\text{BaCl}_n]^{2-n}$ , ( $n = 4-6$ ). All the observed behavior proved once again that complex

ions are formed during mixing of BaCl<sub>2</sub> with CsCl. These good results on high conductivity and low viscosity, proves once again that these HTILs are promising candidates as electrodeposition media.

## Supplementary Information

Supplementary information is available free of charge at <http://jbcs.s bq.org.br> as PDF file.

## Acknowledgments

The work was performed within the research program of the IPC, “Electrode processes, corrosion and materials for electrochemical systems” within the theme “Ionic liquids: properties and electrochemical applications”.

## Author Contributions

The authors AMP and VC contributed equally to the realization of this work.

## References

- Reddy, R. G.; *J. Phase Equilib. Diffus.* **2011**, *32*, 269.
- Caraballo, A.; Galan-Casado, S.; Caballero, A.; Serena, S.; *Energies* **2021**, *14*, 1197.
- Xu, X.; Wang, X.; Li, P.; Li, Y.; Hao, Q.; Xiao, B.; Elsentriecy, H.; Gervasio, D. J.; *Sol. Energy Eng.* **2018**, *140*, 051011.
- Tamaki, S.; Matsunaga, S.; Kusakabe, M. In *Electromagnetic Field Radiation in Matter*; Fano, W. G.; Razzitte, A.; Larocca, P., eds.; IntechOpen: London, UK, 2020, DOI: 10.5772/intechopen.91369.
- Dimitrov, V. I.; *J. Non-Cryst Solids* **2005**, *352*, 216.
- Sharma, S.; Ivanov, A. S.; Margulis, C. J.; *J. Phys. Chem. B* **2021**, *125*, 6359.
- Wang, X.; Chi, Y.; Mu, T.; *J. Mol. Liq.* **2014**, *193*, 262.
- Zuca, S.; Olteanu, M.; Borcan, R.; Popescu, A. M.; Ciochina, M.; *Chem. Pap.* **1991**, *45*, 585.
- Zuca, S.; Borcan, R.; *Rev. Roum. Chim.* **1984**, *20*, 223.
- Popescu, A. M.; *Rev. Roum. Chim.* **1999**, *44*, 765.
- Janz, G. J.; *J. Phys. Chem. Ref. Data* **1980**, *9*, 791.
- Zuca, S.; Borcan, R.; *Rev. Roum. Chim.* **1970**, *15*, 1681.
- Popescu, A. M.; Constantin, V.; *Chem. Res. Chin. Univ.* **2015**, *31*, 858.
- Murgulescu, I. G.; Zuca, S.; *Z. Phys. Chem (Leipzig)* **1961**, *218*, 379.
- Popescu, A. M.; Constantin, V.; *Chem. Eng. Commun.* **2015**, *202*, 1703.
- Fouque, Y.; Gaune-Escard, M.; Szczepaniak, W.; Bogacz, A.; *J. Chim. Phys.* **1978**, *75*, 361.
- Janz, G. J.; *J. Phys. Chem. Ref. Data* **1988**, *17*, (Suppl 2), 1.
- Chhotaray, P. K.; Jella, S.; Gardas, R. L.; *J. Chem. Thermodyn.* **2014**, *74*, 255.
- Glasser, L.; *J. Solid State Chem.* **2013**, *206*, 139.
- Hayyan, A.; Mjalli, F. S.; Al Nashef, I. M.; Al-Wahaibi, T.; Al-Wahaibi, Y. M.; Hashim, M. A.; *Thermochim. Acta* **2012**, *541*, 70.
- Ghatee, M. H.; Zare, M.; Moosavi, F.; Zolghadr, A. R.; *J. Chem. Eng. Data* **2010**, *55*, 3084.
- Zuca, S.; Costin, R.; *Rev. Roum. Chim.* **1970**, *75*, 1831.
- Murgulescu, I. G.; Misdolea, C.; *Rev. Roum. Chim.* **1977**, *22*, 1433.
- Bockris, J. O'M.; Reddy, A. R.; *Modern Electrochemistry*; Plenum Press: NY, USA, 1970, ch. 6.
- Abbott, A. P.; Boothby, D.; Capper, G.; Davies, D. L.; Rasheed, R.; *J. Am. Chem. Soc.* **2004**, *126*, 9142.
- Bonhote, P.; Dias, A. P.; Armand, M.; Papageorgiou, N.; Kalyanasundaram, K.; Gratzel, M.; *Inorg. Chem.* **1996**, *35*, 1168.
- Eyring, H.; John, M. S.; *Significant Liquid Structure*; Wiley: NY, USA, 1969.
- Mateiko, Z. A.; Yagubian, E. S.; Bukhalova, G. A.; *Zh. Neorg. Khim.* **1966**, *11*, 2405.
- Roewer, G.; Emons, H. H.; *Z. Anorg. Allg. Chem.* **1969**, *370*, 128.
- Papatheodorou, G. N.; Ostvold, T.; *J. Phys. Chem.* **1974**, *78*, 181.
- Davis, H. T.; *J. Phys. Chem.* **1972**, *76*, 1629.
- Lumsden, J.; Franzosini, P.; Rolla, M.; Riccardi, M.; Grojtheim, K.; *Discuss. Faraday Soc.* **1961**, *32*, 97.
- Lumsden, J.; *Thermodynamic of Molten Salt Mixtures*; Academic Press: New York, USA, 1966.
- Wang, M.; Wang, C. C.; Cai, H. Q.; Li, Y. Y.; Zhang, Q. W.; Yi, H. B.; *J. Mol. Liq.* **2019**, *274*, 261.
- Li, Y. Y.; Wang, M.; Wang, C. C.; Zhang, Q. W.; Yi, H. B.; *J. Molec. Liq.* **2020**, *314*, 113619.
- Kubota, K.; Tamaki, K.; Nohira, T.; Goto, T.; Hagiwara, R.; *Electrochim. Acta* **2010**, *55*, 1113.
- Angell, C. A. In *Molten Salts and Ionic Liquids: Never the Twain?*; Gaune-Escard, M.; Seddon, K. R., eds.; Wiley: Chichester, UK, 2010.
- Ohno, H.; *Electrochemical Aspects of Ionic Liquids*, 2<sup>nd</sup> ed.; Wiley: New Jersey, USA, 2011.
- Yoshizawa, M.; Xu, W.; Angell, C. A.; *J. Am. Chem. Soc.* **2003**, *125*, 15411.
- Wu, T. Y.; Su, S. G.; Lin, Y. C.; Wang, H. P.; Lin, M. W.; Gung, S. T.; Sun, I. W.; *Electrochim. Acta* **2010**, *56*, 853.
- Olteanu, M.; Pavel, P. M.; *Chem. Pap.* **1999**, *53*, 6.

Submitted: August 20, 2021

Published online: December 6, 2021

